PFC/JA-88-11

Observation of Trapped Particle Modes in a Tandem Mirror

Gerver, M.J.; Golovato, S.N.; Irby, J.H.; Kesner, J.;
Guss, W.C.; Horne, S.F.; Lane, B.G.; Machuzak, J.S.;
Post, R.S.; Sevillano, E.; Zielinski, J.

April 1988

Plasma Fusion Center
Massachusetts Institute of Technology
Cambridge, Massachusetts 02139 USA

Submitted for publication in: The Physics of Fluids

Observation of Trapped Particle Modes in a Tandem Mirror

M.J. Gerver, S.N. Golovato, J.H. Irby, J. Kesner, W.C. Guss, S.F. Horne
B.G. Lane, J.S. Machuzak, R.S. Post, E. Sevillano, J. Zielinski
Plasma Fusion Center
Massachusetts Institute of Technology
Cambridge , Massachusetts 02139

ABSTRACT

An instability with $m \geq 3$ localized to an axisymmetric end cell of the Tara tandem mirror has been observed, most prominently during strong ICRF heating in the end cell. The instability, which causes enhanced radial losses, becomes either more stable or flutelike when the connection (passing fraction) between the central cell and end cell is increased, depending on whether sufficient stabilization is provided in the central cell. The beta is sufficiently low to rule out the possibility of MHD ballooning modes. Based on the plasma parameters, the instability appears to be a collisionless trapped particle mode that has been predicted to be unstable in linked minimum and maximum B mirror devices.

I. Introduction

Trapped particle modes were proposed by Kadomtsev and Pogutse in 1970[1] to be a serious limitation in devices containing a class of particles that are trapped in a region of bad magnetic curvature. These modes are basically electrostatic and thus can exist at low beta. Berk et al.[2] pointed out that a virulent form of collisionless trapped particle mode exhibiting magnetohydrodynamic (MHD) growth rates should occur in tandem mirrors when there is insufficient electrical connection between adjacent stable and unstable mirror cells. The high growth rate of this instability comes about because of the absence in open ended devices of stabilizing passing particles that are present in toroidal devices with rotational transform. However, these modes may be stabilized by a sufficient fraction of particles that pass between the stable and unstable cells. Typically the unstable cell is a maximum-B (bad curvature) mirror and the stable cell is a minimum-B (good curvature) mirror.

The collisionless trapped particle mode has been identified in low temperature plasmas in small linked-mirror-cell devices.[3,4] However this instability has not previously been clearly identified in the parameter regimes achieved by larger confinement devices, although there has been some recent speculation[5,6] that instabilities seen in TMX-U[5-7] may have been collisionless trapped particle modes. (In addition, collisional $m = 1$ trapped particle modes were probably associated with radial losses in the central cell of TMX[8] and TMX-U.[9])

In this article we describe the excitation of a trapped particle mode during plugging experiments in the Tara tandem mirror device.[10,11]The mode appeared when a sufficiently high mirror ratio separated the stable central cell from the unstable axisymmetric plugging cell, termed the axicell. In Tara the central cell was stabilized not by good curvature, but by the ponderomotive force that accompanied ion cyclotron resonance frequency (ICRF) heating, and by a magnetic divertor.[10,11,12] When strong ICRF power was applied in the axicell a localized sawtooth behavior in the diamagnetism and density was observed. The sawtooth dumps were preceded by the growth of a fluctuation with MHD-like frequency and azimuthal mode number $m \geq 3$. The adjacent central cell remained virtually unaffected although a very small motion of the central cell plasma sometimes accompanied the strong axicell dumps. Modes at MHD-like frequencies and high azimuthal mode number were also observed in the axicell when electron cyclotron heating (ECH) power or neutral beams were applied, although sawteeth were not seen then.

Section II will describe the experimental setup and the key diagnostics. Section III contains experimental results and Sec. IV the conclusions.

II. Experimental Setup

Experiments were performed in the Tara tandem mirror. The magnetic geometry of this device is shown in Fig. 1. The central cell was maintained by ICRF excitation and gas fueling on a local magnetic hill at the central cell midplane (at B = 4 kG).[13] A slot antenna launched slow waves that propagated into the gradient and heated near the local wells on either side of the midplane at a field of B $\simeq$ 2 kG. The magnetic divertor was also located on the midplane magnetic hill.

The central cell was bounded on either side by axisymmetric mirror cells (axicells), which had a mirror ratio of 5. In the experiments discussed here the north axicell was heated by ICRF launched from an antenna located within the cell on the outer magnetic hill at a mirror ratio of 2. In some shots ECH or neutral beam heating was used in addition to or instead of ICRF. On the outside, the axicells connected through a transition regions into quadrupole cells termed anchors. No plasma pressure was built up in the north anchor during these experiments. In some of the experiments the south anchor was also heated by ICRF to provide some additional MHD stability.

All of the mirror cells contained diamagnetic loops to measure stored plasma energy, and microwave interferometers to measure line density. Double-tipped Langmuir probes were used in the north axicell to measure azimuthal mode number. Other important diagnostics were :

1. Near UV continuum and Hα detector arrays (8 or 16 chords), termed plasma position detectors (PPD), located in the central cell and in the axicell, that monitored the motion of the plasma centroid.
2. A 140 GHz gyrotron scattering diagnostic[14,15] located at the north axicell midplane. This diagnostic detects microwaves scattered off density fluctuations in the bandwidth of 0 to 100 MHz at $k_\perp$ = 0.9, 22 and 41 cm^{-1}.
3. A heavy ion beam probe located in the south central cell. As well as measuring the local potential, it was also a sensitive detector of local density fluctuations.

III. Experimental Results

In the absence of anchor stabilization the central cell could be stabilized by a combination of ponderomotive stabilization (which was observed to be proportional to the ICRF power) and the action of the magnetic divertor[12]. The central cell fluctuation level observed on the interferometers was less than 10% . Typical central cell parameters were $T_e \approx$ 60 eV, $T_{i\perp} \approx$ 500-800 eV, $T_{i\parallel} \approx$ 200 eV. The density profile was gaussian with an

8-13 cm half-width and the limiter was located at 20 cm. ICRF power was applied in both the central cell and the adjoining north axicell. The electrical connection between these cells (determined by the fraction of passing particles) was controlled by varying the central cell mirror ratio R_c from 6 to 12.

Flute-like Modes

For a low mirror ratio there was good electrical connection between cells, which suppressed localized modes when the central cell was strongly stabilized. When the stability of the central cell was decreased, by reducing the current in the magnetic divertor for example, $m = 1$ or $m = 2$ flute-like instabilities were produced.

Such a case with an $m = 1$ mode is illustrated in Fig. 2 for a reduced central cell mirror ratio, $R_c = 7$. Here ICRF was applied in the north axicell at t= 20 ms. The divertor current was reduced by 5% which reduced the stability of the central cell-axicell system. In Fig. 2a we observe the north plug diamagnetism drop 15% and then recover (t=22.8 ms), 36% and then recover (t=23.6 ms), and then drop 74% and remain low (t=24.7 ms). At the same times (Fig. 2b) the central cell diamagnetism drops 6%, 13% and 37% while the centroid moves 2.4 cm, 3.5 and 8.3 cm respectively. Clearly more plasma was scraping off as it moved farther off axis, and for a large enough amplitude centroid motion the plasma entered a continuously unstable state.[16] Although it has not been shown that the perturbed potential of this mode was exactly the same in the central cell and the north axicell, it is clear that the mode had a substantial amplitude in both the central cell and the north plug, and in this qualitative sense it was "flute-like". On similar shots where the axicell PPD was used, $m = 1$ or $m = 2$ central cell modes were measured simultaneously in the axicell.

Trapped Particle Modes

At the highest divertor currents and at high R_c, ICRF heating in the north axicell was observed to drive only the axicell unstable. A buildup and dump in density and diamagnetism (beta) was observed to occur with 1 to 2 ms periodicity. During each dump the neutral density increased in the axicell (as seen by the axicell PPD and other diagnostics), indicating that the plasma was scraping off in the axicell. These "sawteeth" and the increases in neutral density were *not* observed in the central cell. Fig. 3 shows the central cell and north axicell diamagnetism and line density for such a shot. The sawteeth are seen in the north axicell only.

Fig. 4 shows an expanded view of one of the sawteeth. We observe from the gyrotron

scattering signal that the axicell diamagnetism rise triggers a coherent low frequency burst ($\approx$ 30 kHz) which builds up until the dump. A correlated burst could be detected by the central cell heavy ion beam probe only in shots where the instability was most strong. Absolute calibration of these two diagnostics is not known sufficiently well to determine the relative amplitudes. The 30 kHz signal was generally *not* seen on the axicell PPD, a line integrated diagnostic that should be insensitive to high m modes. Since the axicell PPD did pick up $m = 1$ and $m = 2$ flutelike modes, this suggests that the 30 kHz mode had $m \geq 3$. (The 30 kHz mode was occasionally seen on the axicell PPD in shots with very large sawteeth, but at $m = 0$, due to the modulation of the plasma light emission by the release of neutral gas when the plasma periodically scraped off.)

Figure 5 shows that the sawteeth decreased in amplitude and frequency as the mirror ratio between the central cell and axicell was decreased. This data was taken at maximum central cell divertor current. This result was also checked by varying the axicell outer high field coils. This variation did not affect the appearance of the sawteeth, showing that it is the connection to the central cell that is important, not the axicell mirror ratio.

Azimuthal Mode Number

MHD ballooning is precluded by a relatively small axicell beta (less than 1%) and the passing fraction dependence implies that we are observing a trapped particle mode. Theoretically,[2] cancellation between the ion finite Larmor radius (FLR) stabilization term and the collisionless trapped particle mode charge separation term should lead to an unstable band of modes for azimuthal mode numbers close to

$$m^2 - 1 = \frac{L_c}{L_c + L_{ax}} \frac{n_{pass}}{n_e} \left(\frac{a}{\rho_i}\right)^2 \qquad (1)$$

with L_c and L_{ax} respectively the central cell and axicell length, n_{pass}/n_e the fraction of electrons in the axicell which pass into the central cell, a the plasma radius and ρ_i the ion gyroradius. In Tara, neglecting collisions is valid for this range of m if the relevant collision frequency is the Pastukhov rate. For $a/\rho_i \approx 20$ and $n_{pass}/n_e \approx 0.1$ we obtain $m \approx 4$ to 5. The data in Fig. 5 showed that the sawteeth decreased in amplitude when the passing fraction n_{pass}/n_e was increased by decreasing the mirror ratio between the central cell and axicell. According to Eq. (1), the azimuthal mode number m at which trapped particle modes are unstable is an increasing function of passing fraction. We expect that modes with higher m will cause less rapid radial transport, since the radial loss rate is probably roughly γ/m^2 (where γ is the linear growth rate), and hence they will cause smaller sawteeth. The clear dependence of the sawtooth amplitude on passing fraction is

an important signature of a trapped particle mode.

Measurements were made with a double-tipped Langmuir probe in the north axicell to establish the azimuthal mode number of the instability. The unstable mode modulated the coupling of the ICRF to the plasma (and hence to the probes), so any nonlinearity in the probes produced a spurious signal at the mode frequency but with a different phase, making it impossible to measure the phase of the mode. Therefore, in probe experiments, the ICRF in the central cell, axicell, and anchors was briefly turned off while the measurement was made. This tended to make the central cell go unstable with an $m = 1$ mode at about 10 kHz, but the higher frequency modes (25-100 kHz) seen in the axicell persisted for a few hundred μs, without much change in frequency or amplitude, after the ICRF was turned off. Thus we assume that the azimuthal mode numbers were the same when the ICRF was on. When neutral beams or ECH were used to drive the axicell, they could be kept on during measurement of azimuthal mode numbers. Fig. 6 shows typical results indicating an $m = 3$ mode at 32 kHz and an $m = 8$ mode at 54 kHz, for a shot where axicell neutral beams were used. (The 13 kHz mode also seen in Fig. 6 is not a trapped particle mode, but has been identified as an $m = 0$ ion acoustic mode, transiently excited by the sudden removal of ponderomotive force from the south half of the central cell, with a 180° phase difference between the north and south ends of the central cell. A similar mode was seen in TMX.[8]) Measurements of parallel wave number $k_{\|}$ were also made with the double-tipped Langmuir probe in the north axicell, and showed that $k_{\|} \ll k_{\perp}$ for these modes, as expected.

IV. Discussion and Conclusions

We have observed that localized plasma dumps in the maximum-B axicells accompanied strong axicell ICRF heating when the mirror ratio between the axicell and the central cell was sufficiently high. The accompanying 25-100 kHz oscillations imply that trapped particle modes were present. Measurements of moderately high azimuthal mode numbers and of a clear dependence on mirror ratio (and therefore passing fraction) support the contention that we were observing trapped particle modes. Lowering the mirror ratio to the central cell either reduced the mode amplitude, or led to flute-like instability, depending on the amount of stability provided in the central cell.

Similar modes were seen when the axicell was heated by neutral beams or by ECH, although in these cases the axicell diamagnetism did not exhibit sudden dumps ("sawteeth"), but had steady enhanced radial losses. The maximum diamagnetism that we were able to obtain in the axicell was about the same (when weighted by bad curvature and averaged over the length of the axicell) for ICRF, ECH, and neutral beam heating, and

was much lower than the diamagnetism that has been obtained using comparable heating power in other mirror experiments with minimum-B cells, such as Constance[17] and TMX-U.[18] The saturation in diamagnetism seen in Tara may very well be due to the enhanced radial losses caused by trapped particle modes.[19] In addition to explaining the saturation in diamagnetism, these enhanced radial losses can explain certain features of the central cell particle balance and the axicell electron distribution function during ECH.[20]

The enhanced radial loss rate needed to explain the saturation in axicell diamagnetism can be determined by taking the ratio of the initial rate of rise of diamagnetism (before trapped particle modes set in) to the diamagnetism at saturation. The heating rate was typically about $3 \times 10^3 s^{-1}$, comparable to the radial loss rate γ_{mhd}/m^2 theoretically estimated for trapped particle modes. If the radial loss rate were a function only of the diamagnetism, then one might expect the diamagnetism to approach a steady saturated level, and indeed this did occur when neutral beam heating was used. With ICRF, on the other hand, the diamagnetism generally oscillated around a steady state, exhibiting sawteeth. During the rising phase of a sawtooth, the rate of rise of diamagnetism was comparable to what it was at the onset of heating, suggesting that trapped particle modes were completely stable during the rising phase, while during the falling phase at the same diamagnetism they were evidently very unstable with linear growth rate comparable to an MHD growth rate. As may be seen from Fig. 5, this was true regardless of the size of the sawteeth, which suggests that the failure to reach a steady state was not due simply to the large amplitude of trapped particle modes during ICRF, but to some qualitative difference between ICRF and neutral beam heating. Possible candidates for this difference are the ponderomotive force associated with ICRF, and the anisotropy of the ion distribution during ICRF. If the anisotropy and β were great enough, the ions would be subject to an Alfven ion cyclotron instability[21] which would spread them out in pitch angle in a time short compared to the trapped particle mode growth time. This in turn would increase the drive for the trapped particle modes, because the magnetic curvature in the axicell was locally an increasing function of distance from the midplane. There is some evidence from the gyrotron scattering diagnostic, as well as from probes, that an Alfven ion cyclotron instability appeared in the axicell as a precursor to sawteeth.[14]

The enhanced radial losses caused by trapped particle modes severely limited the diamagnetism that could build up in the axicell, even when the central cell was very stable. Complete stability to trapped particle modes, and the consequent possibility of obtaining high diamagnetism in an axicell, would be possible only if the passing fraction were extremely high, so that the passing particles would contribute significantly to the MHD drive term; or, more in keeping with the concept of a tandem mirror, if the axicell were stabilized locally, by a magnetic divertor, ponderomotive force, cusps, or some other

means.

Acknowledgements

This work was performed under U.S. DOE contract DE-AC02-78ET51013. We are grateful to K. Brau and J. A. Casey (MIT), T. A. Casper and L.D. Pearlstein (LLNL), M. E. Mauel (Columbia), and G. A. Hallock (U. of Texas) for useful discussions.

References:

[1] B. B. Kadomtsev and O. P. Pogutse, Nucl. Fus. **11**, 67 (1970).

[2] H. L. Berk, M. N. Rosenbluth, H. V. Wong, T. M. Antonsen and D. E. Baldwin, Fiz. Plasmy **9**, 176 (1983) [Sov. J. Plasma Phys. **9**, 108 (1983)].

[3] R. Scarmozzino, A. K. Sen, G. Navratil, Phys Rev Letters **57**, 1729 (1986).

[4] J. C. Fernandez, C. P. Chang, A. J. Lichtenberg , M. A. Lieberman and H. Meuth, Phys. Fluids **29**, 1208 (1986).

[5] T. A. Casper, in "TMX-U Final Report" (G. D. Porter, ed.), LLNL Report UCID-20981 Vol. 2, February 1, 1988, Sec. 7.1 and 7.2.3.

[6] T. C. Simonen, H. L. Berk, and T. A. Casper, "MHD Stability Analysis of the Tandem Mirror Experiment-Upgrade," *ibid.*, Sec. 7.2.2, submitted to Nuclear Fusion (1988).

[7] T. A. Casper, L. Z. Berzins, E. B. Hooper, and G. F. Campbell, Bull. Am. Phys. Soc. **30**, 1434 (1985).

[8] E. B. Hooper, Jr., G. A. Hallock, and J. H. Foote, Phys. Fluids **26**, 314 (1983).

[9] J. Marilleau, T. A. Casper, E. B. Hooper, A. W. Molvik, and A. K. Sen, Bull. Am. Phys. Soc. **29**, 1393 (1984).

[10] J. Kesner, R. S. Post, B. D. McVey, D. K. Smith, Nucl. Fusion **22**, 549 (1982).

[11] R. S. Post, M. Gerver J. Kesner, J. H. Irby, B. G. Lane, et al., *Plasma Physics and Controlled Nuclear Fusion Research*, 1984, London (IAEA, Vienna, 1985), Vol. II, p. 285.

[12] J. Casey, B. Lane, J. H. Irby, K .L. Brau, S. N. Golovato, W. C. Guss, J. Kesner, R. S. Post, E. Sevillano and J. Zielinski, "Experimental Studies of Divertor Stabilization in an Axisymmetric Tandem Mirror, MIT Rept. PFC/JA-87-25 (1987), submitted to Phys. Fluids (1988).

[13] S. N. Golovato, K. Brau, J. Casey, J. W. Coleman, M. J. Gerver, et al., "Plasma Production and Heating by ICRF in the Central Cell of the Tara Tandem Mirror", MIT Report PFC/JA-88-15 (1988), to be submitted to Phys. Fluids.

[14] J. S. Machuzak, R. C. Myer, P. Woskoboinikow, D. R. Cohn, M. Gerver, S. N. Golovato, S. Horne, S. Kubota, W. J. Mulligan, R. S. Post, D. Rhee, and R. J. Temkin, "Gyrotron Scattering from Non-Thermal Fluctuations in the Tara Tandem Mirror", *Conference Digest*

of Twelth International Conference on Infared and Millimeter Waves, December 14-18, 1987, Lake Buena Vista (Orlando), Florida (IEEE, New York, 1987).

[15] J. S. Machuzak, P. Woskoboinikow, W. J. Mulligan, D. R. Cohn, M. Gerver, W. Guss, M. Mauel, R. S. Post, and R. J. Temkin, Rev. Sci. Instr. **57**, 1983 (1986).

[16] J. H. Irby, B. G. Lane, J. A. Casey, K. Brau, S. N. Golovato, W. C. Guss, S. F. Horne, J. Kesner, R. S. Post, E. Sevillano, J. D. Sullivan, and D. K. Smith, Phys. Fluids **31**, 902 (1988).

[17] Xing Chen, B. G. Lane, D. L. Smatlak, R. S. Post, and S. A. Hokin, "Experimental Study of the Hot Electron Plasma Equilibrium in the Constance B Mirror Experiment", to be published in Phys. Fluids (1988); D. L. Smatlak, X. Chen, B. G. Lane, S. A. Hokin, R. S. Post, Phys. Rev. Lett. **58**, 1853 (1987).

[18] T. J. Orzechowski, S. L. Allen, J. H. Foote, R. K. Goodman, A. W. Molvik, and T. C. Simonen, Phys. Fluids **26**, 2335 (1983); T. C. Simonen et al., in *Plasma Physics and Controlled Nuclear Fusion Research*, 1984, London (IAEA, Vienna, 1985), Vol. II, p. 255; B. W. Stallard, W. F. Cummins, A. W. Molvik, P. Poulsen, T. C. Simonen, S. Falabella, J. D. Barter, T. Christensen, G. Dimonte, and T. E. Romesser, in *Proc. 4th Int. Symp. Heating Toroidal Plasmas, Rome, Italy, 1984* (International School of Plasma Physics, Varenna, Italy, 1984) Vol. 2, p. 931.

[19] The diamagnetism did not saturate when $2\omega_{ce}$ ECH was used, due to the buildup of hot electrons, which should not be affected by trapped particle modes if their drift frequency is greater than the mode frequency. The *warm* electron diamagnetism did saturate.

[20] M. J. Gerver, W. C. Guss, S. F. Horne, and X. Z. Yao, Bull. Am. Phys. Soc. **32**, 1882 (1987).

[21] G. R. Smith, Phys. Fluids **27**, 1499 (1984), and references therein.

Figure Captions:

FIG. 1. Tara configuration showing the axial magnetic field.

FIG. 2. a) North plug diamagnetism, b) central cell diamagnetism and c) central cell centroid location respectively vs. time for a low mirror ratio experiment that exhibits an interchange mode.

FIG. 3. North axicell and central cell signals for a shot exhibiting sawtooth behavior that is strongly localized in the north axicell.

FIG. 4. Expanded timescale for North axicell and central cell signals for a shot exhibiting sawtooth behavior that is strongly localized in the north axicell.

FIG. 5. Series of shots exhibiting the damping of the north axicell sawteeth as the central cell mirror ratio R_c, is decreased.

FIG. 6. Signals from two Langmuir probes at r=10 cm separated azimuthally by 1.9 cm, and the cross correlated power spectrum and phase difference between the two signals. The phase difference shows that the mode at 32 kHz is $m = 3$, and the mode at 54 kHz is $m = 8$. The mode at 13 kHz is not a trapped particle mode but an $m = 0$ ion acoustic mode generated in the central cell.

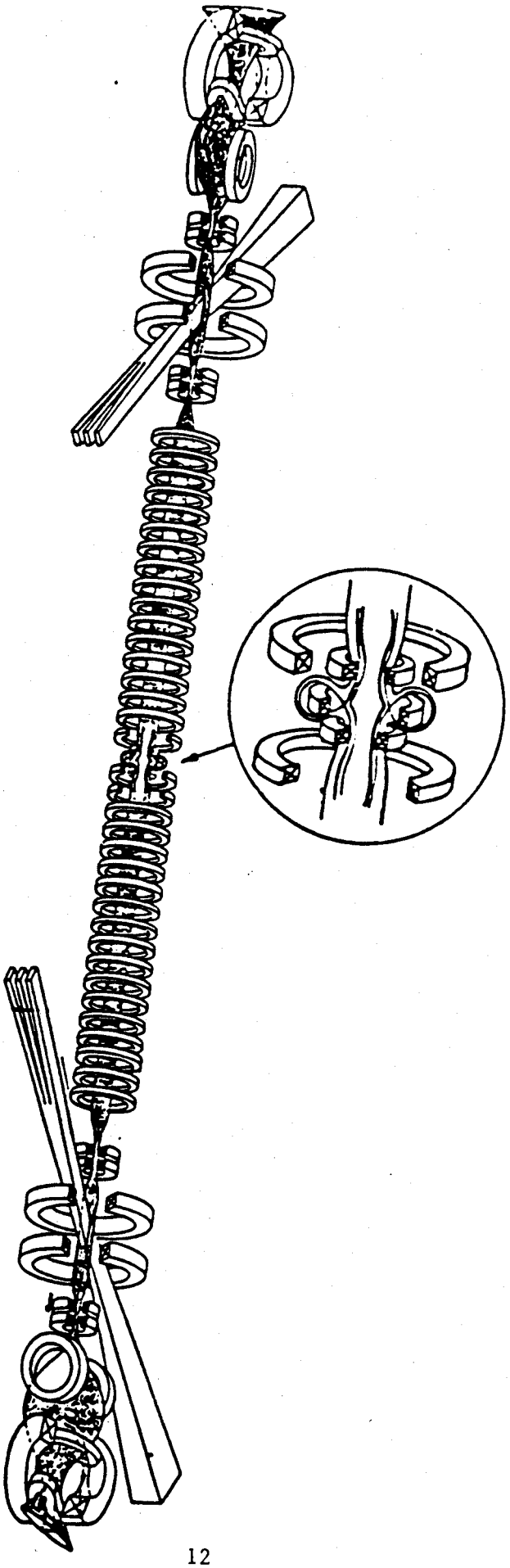

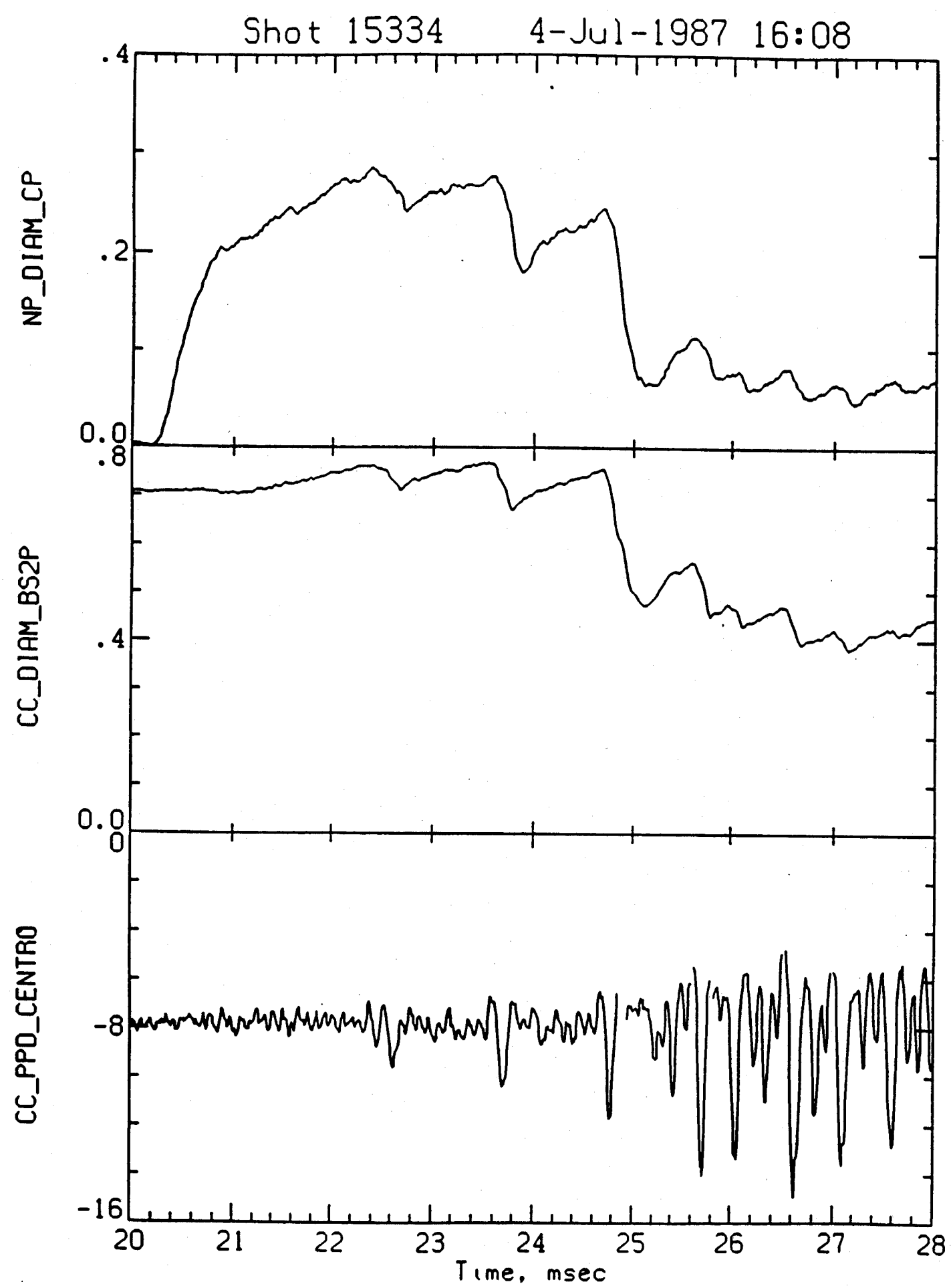
Shot 15334 4-Jul-1987 16:08
NP_DIAM_CP
.4
.2
0.0
CC_DIAM_BS2P
.8
.4
0.0
CC_PPO_CENTRO
0
-8
-16
20
21
22
23
24
25
26
27
28
Time, msec

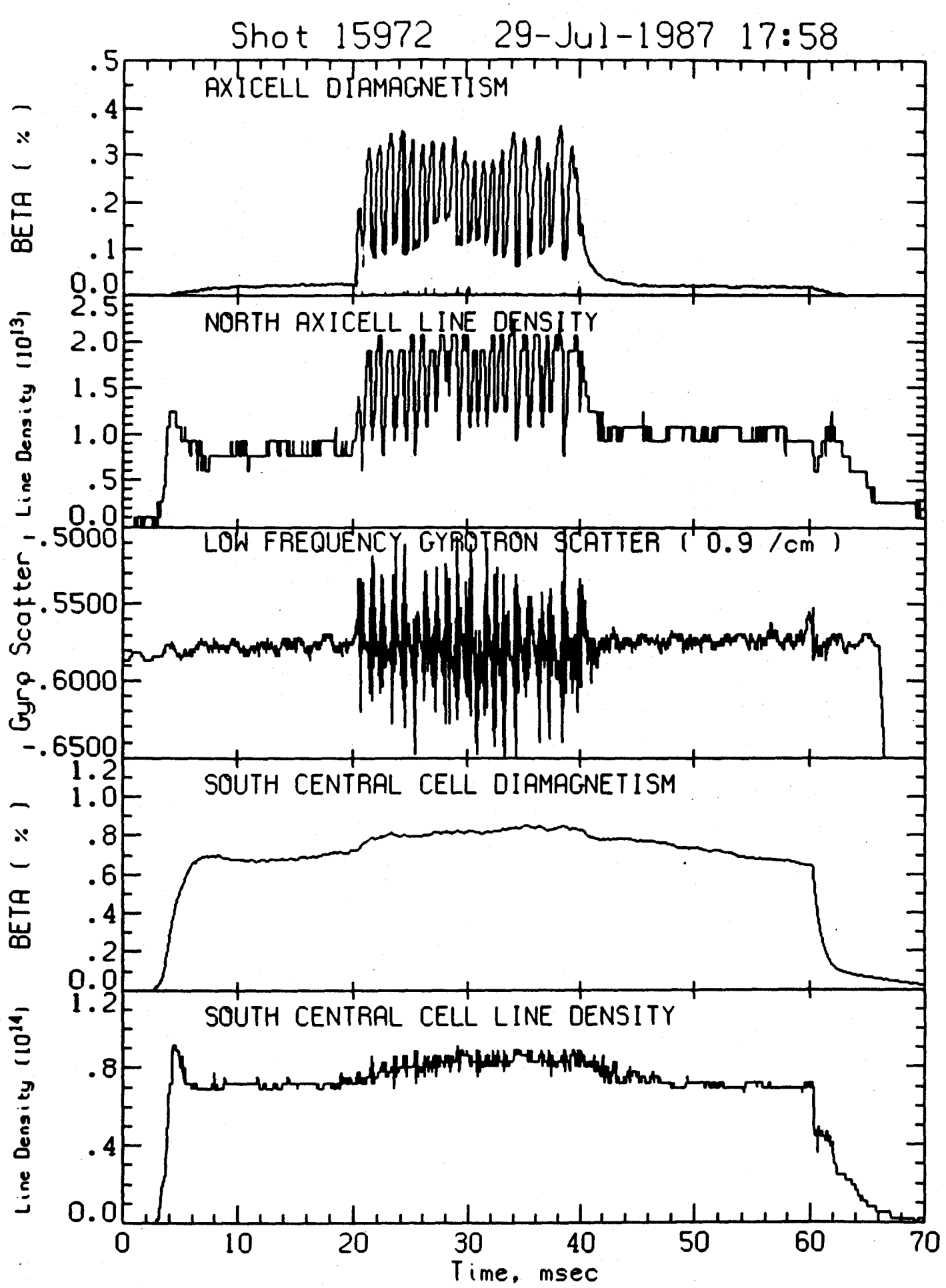
Shot 15972 29-Jul-1987 17:58
AXICELL DIAMAGNETISM
BETA (%)
.5
.4
.3
.2
.1
0.0
NORTH AXICELL LINE DENSITY
Line Density (10^{13})
2.5
2.0
1.5
1.0
.5
0.0
LOW FREQUENCY GYROTRON SCATTER (0.9 /cm)
Gyro Scatter
.5000
.5500
.6000
.6500
SOUTH CENTRAL CELL DIAMAGNETISM
BETA (%)
1.2
1.0
.8
.6
.4
.2
0.0
SOUTH CENTRAL CELL LINE DENSITY
Line Density (10^{14})
1.2
.8
.4
0.0
0
10
20
30
40
50
60
70
Time, msec

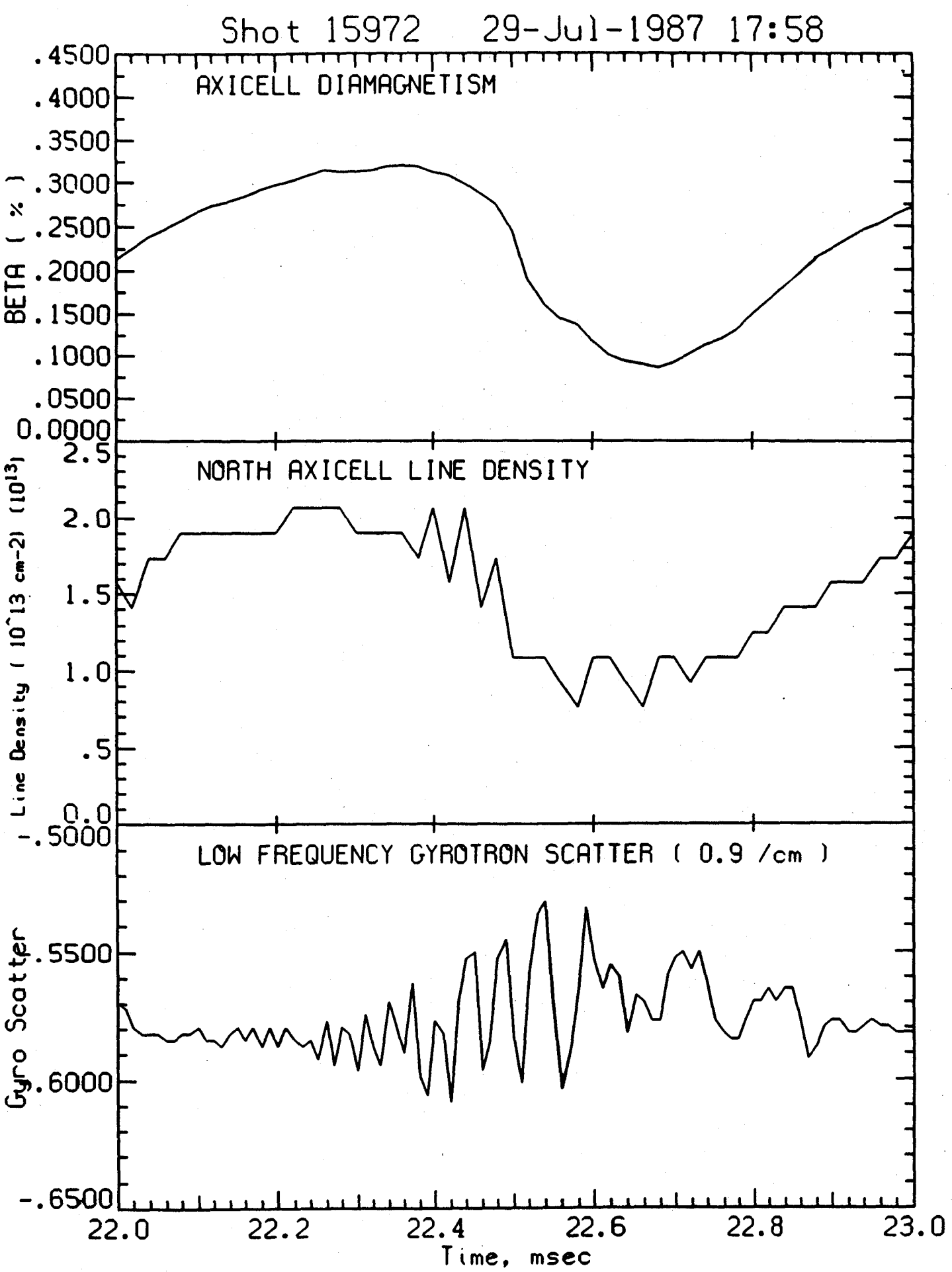
Shot 15972 29-Jul-1987 17:58
AXICELL DIAMAGNETISM
BETA (%)
.4500
.4000
.3500
.3000
.2500
.2000
.1500
.1000
.0500
0.0000
NORTH AXICELL LINE DENSITY
Line Density (10^13 cm-2) (10^13)
2.5
2.0
1.5
1.0
.5
0.0
-.5000
LOW FREQUENCY GYROTRON SCATTER (0.9 /cm)
Gyro Scatter
.5500
.6000
-.6500
22.0
22.2
22.4
22.6
22.8
23.0
Time, msec

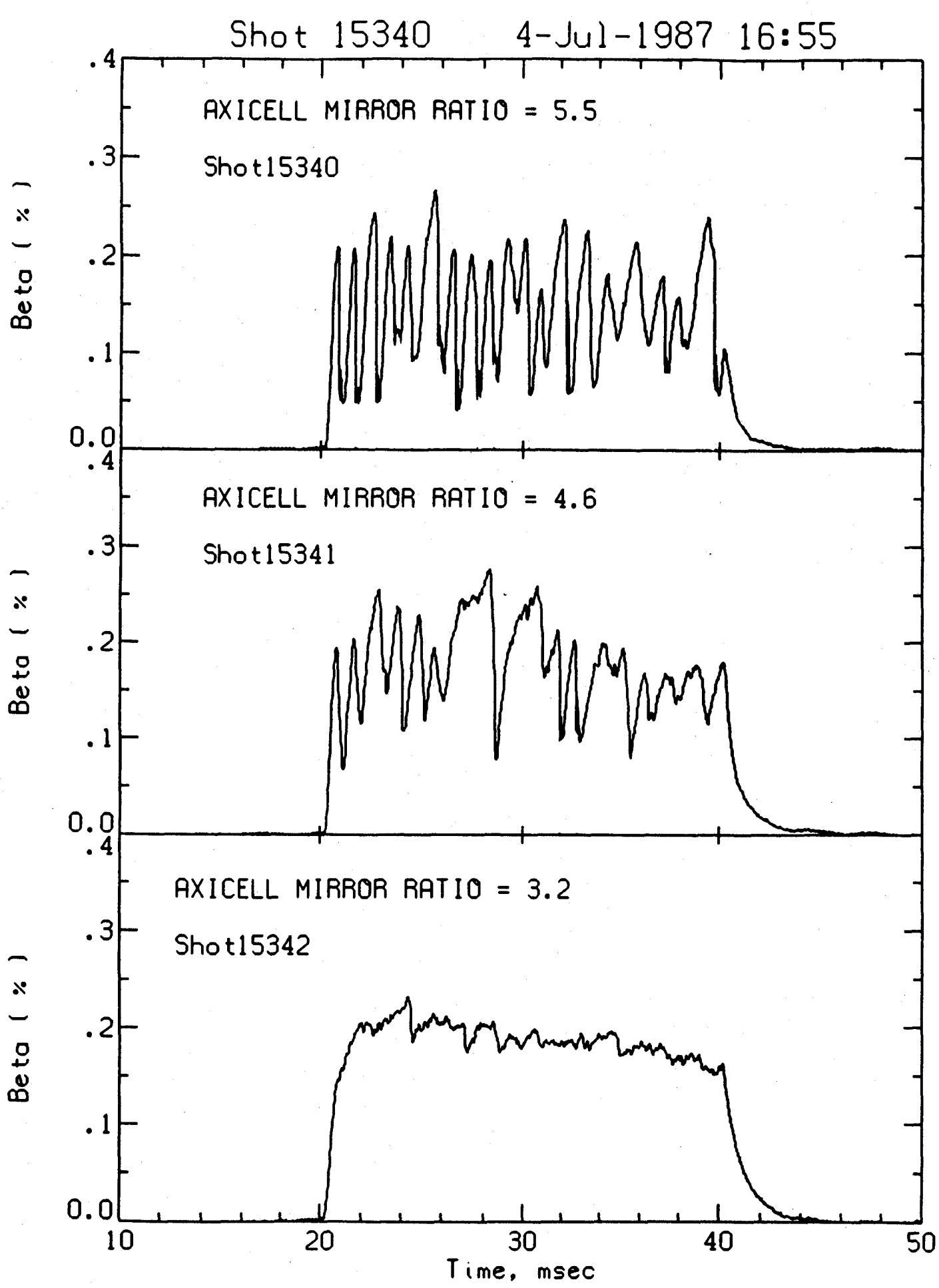
Shot 15340 4-Jul-1987 16:55
AXICELL MIRROR RATIO = 5.5
Shot15340
AXICELL MIRROR RATIO = 4.6
Shot15341
AXICELL MIRROR RATIO = 3.2
Shot15342
Beta (%)
.4
.3
.2
.1
0.0
10
20
30
40
50
Time, msec

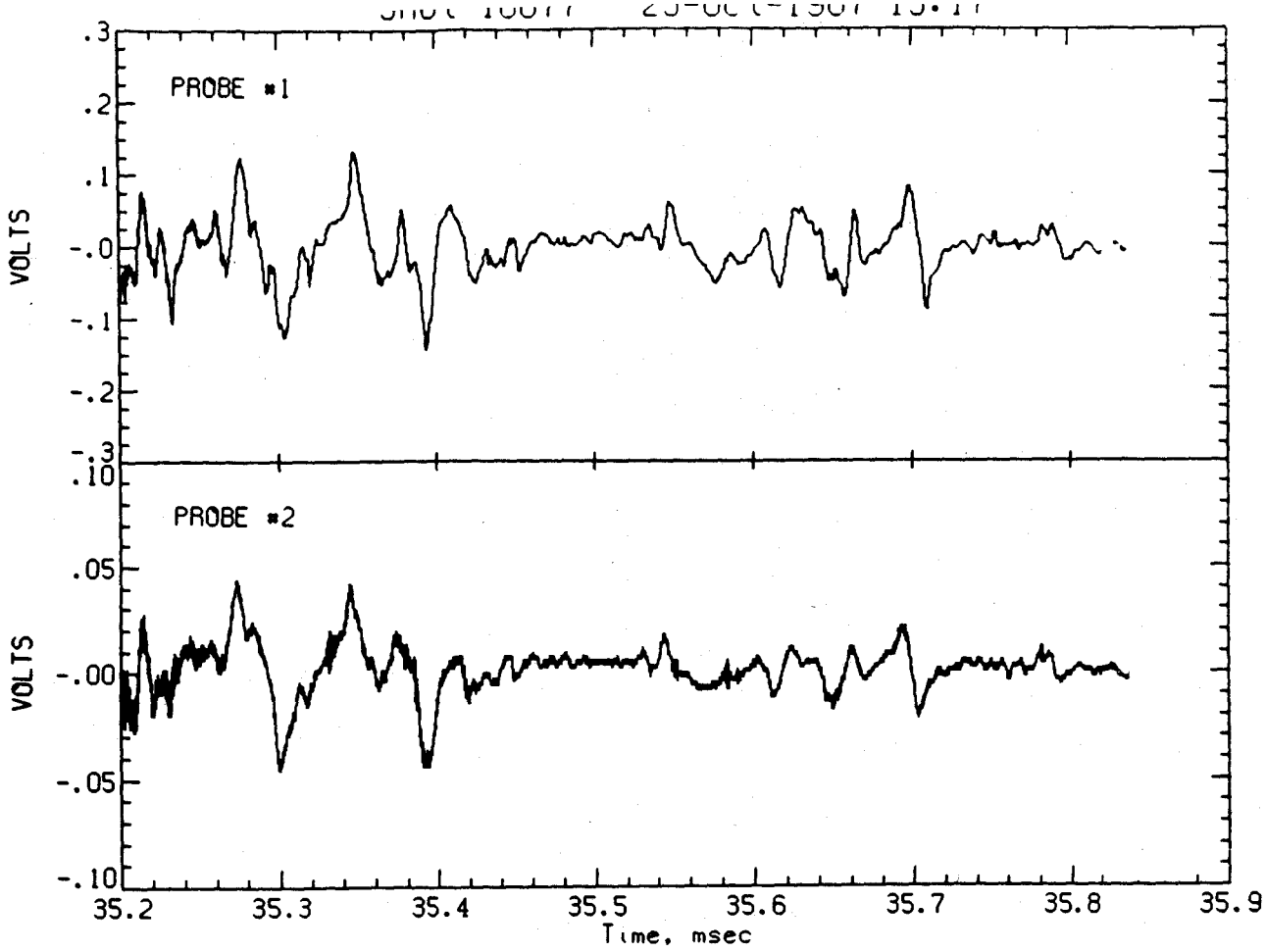
PROBE #1
PROBE #2
VOLTS
VOLTS
.3
.2
.1
-.0
-.1
-.2
-.3
.10
.05
-.00
-.05
-.10
35.2
35.3
35.4
35.5
35.6
35.7
35.8
35.9
Time, msec

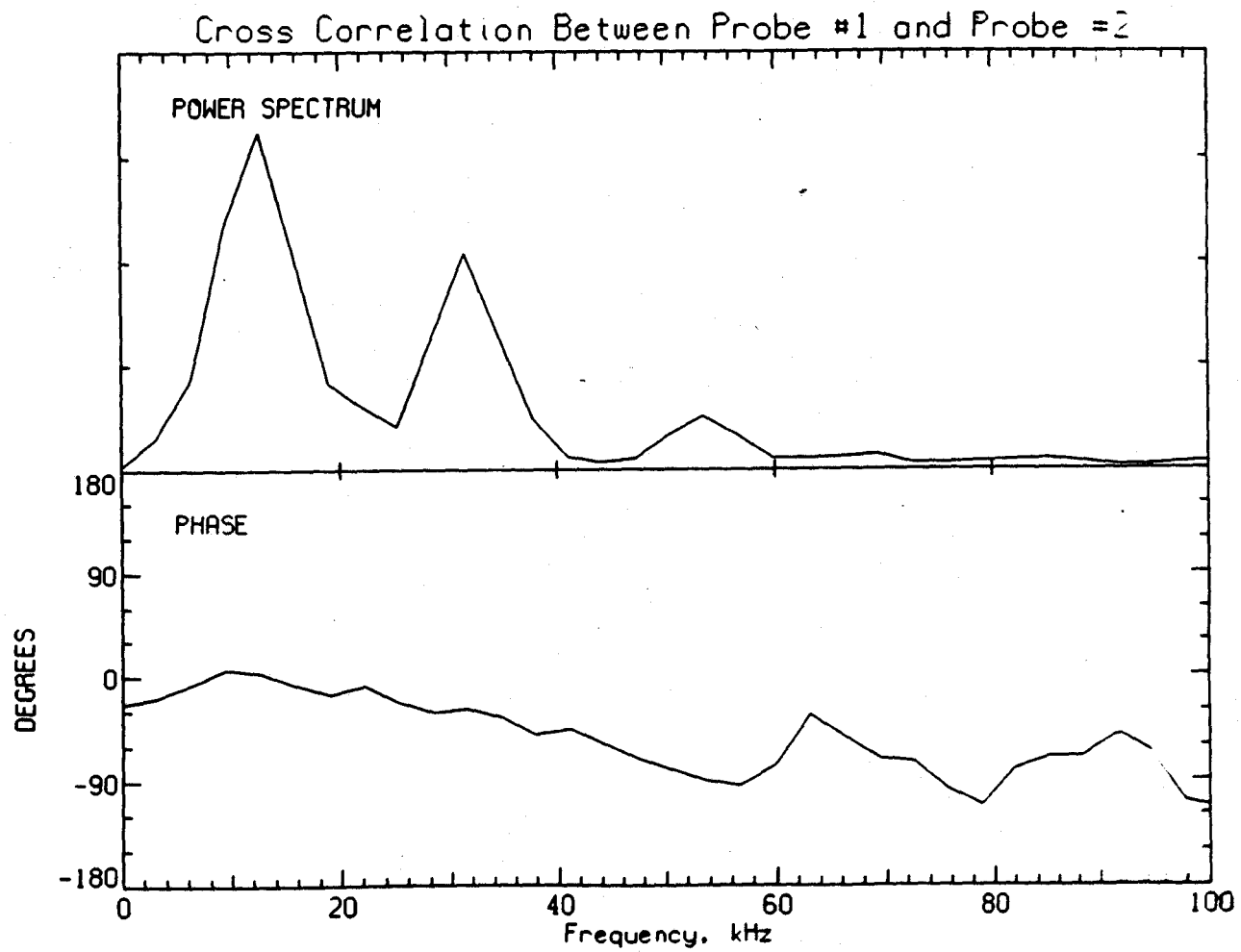
Cross Correlation Between Probe #1 and Probe #2
POWER SPECTRUM
PHASE
DEGREES
180
90
0
-90
-180
0
20
40
60
80
100
Frequency, kHz